Current self-oscillations, spikes and crossover between charge monopole and dipole waves in semiconductor superlattices

David Sánchez[1], Miguel Moscoso[2,3], Luis L. Bonilla[2,3], Gloria Platero[1] and Ramón Aguado[1]

[1]*Instituto de Ciencia de Materiales (CSIC), Cantoblanco, 28049 Madrid, Spain*
[2]*Escuela Politécnica Superior, Universidad Carlos III de Madrid, Avenida de la Universidad 20, 28911 Leganés, Spain.*
[3]*Also: Unidad Asociada al Instituto de Ciencia de Materiales (CSIC)*
(February 1, 2008)

Self-sustained current oscillations in weakly-coupled superlattices are studied by means of a self-consistent microscopic model of sequential tunneling including boundary conditions naturally. Well-to-well hopping and recycling of charge monopole domain walls produce current spikes –high frequency modulation– superimposed on the oscillation. For highly doped injecting contacts, the self-oscillations are due to dynamics of monopoles. As the contact doping decreases, a lower-frequency oscillatory mode due to recycling and motion of charge dipoles is predicted. For low contact doping, this mode dominates and monopole oscillations disappear. At intermediate doping, both oscillation modes coexist as stable solutions and hysteresis between them is possible.

73.40.Gk, 73.50.Fq, 73.50.Mx

Solid state electronic devices presenting negative differential conductance, such as resonant tunneling diodes, Gunn diodes or Josephson junctions [1], are nonlinear dynamical systems with many degrees of freedom. They display typical nonlinear phenomena such as multistability, oscillations, pattern formation or bifurcation to chaos. In particular, vertical transport in weakly coupled semiconductor doped superlattices (SLs) has been shown to exhibit electric field domain formation [2–4], multistability [5], self-sustained current oscillations [6–8], and driven and undriven chaos [9–11]. Stationary electric field domains appear in voltage biased SLs if the doping is large enough [4]. When the carrier density is below a critical value, self-sustained oscillations of the current may appear. They are due to the dynamics of the domain wall (which is a charge monopole accumulation layer or, briefly, a *monopole*) separating the electric field domains. This domain wall moves through the structure and is periodically recycled. The frequencies of the corresponding oscillation depend on the applied bias and range from the kHz to the GHz regime. Self-oscillations persist even at room temperature, which makes these devices promising candidates for microwave generation [7]. Theoretical and experimental work on these systems have gone hand in hand. Thus the paramount role of monopole dynamics has been demonstrated by theory and experiments. Monopole motion and recycling can be experimentally shown by counting the spikes –high frequency modulation– superimposed on one period of the current self-oscillations: current spikes correspond to well-to-well hopping of a domain wall through the SL. In typical experiments the number of spikes per oscillation period is clearly less than the number of SL wells [7,12]. It is known that monopoles are nucleated well inside the SL [7,8] so that the number of spikes tells over which part of the SL they move. Other possible waves, such as the charge dipole waves appearing in the well-known Gunn effect, are nucleated at the emitter contact [13]. Had they been mediating the self-oscillation, the number of current spikes would be comparable that of SL wells.

In this letter we study the non-linear dynamics of SLs by numerically simulating the model proposed in Ref. [14]. Our simulations show self-sustained oscillations of the current and current spikes reflecting the motion of the domain wall as observed experimentally. Furthermore, when contact doping is diminished, we predict a crossover from monopole to dipole self-oscillations resembling those in the Gunn effect [13]. Indeed, our results show for first time that there is an intermediate range of contact doping and a certain interval of external dc voltage for which monopole and dipole self-oscillations with different frequencies are both stable. Hysteretic phenomena then exist.

1. Model and superlattice sample. Our self-consistent microscopic model of sequential tunneling includes a detailed electrostatic description of the contact regions and SL [14]. It consists of a system of $3N + 8$ equations for the Fermi energies and potential drops at the N wells, the potential drops at the barriers and at the emitter and contact layers, width thereof, charge at the emitter and total current density. These equations comprise Ampère current density balance and Poisson equations, conservation of the global charge, and the overall voltage bias condition. Dynamics enters the model through Ampère's law for the total current density $J = J(t)$,

$$J = J_{i-1,i} + \frac{\epsilon}{d} \frac{dV_i}{dt}, \qquad (1)$$

which is equivalent to a local charge continuity equation [14]. Here $J_{i-1,i}$ is the tunneling current density through the ith barrier of thickness d, evaluated by using the Transfer Hamiltonian approach [14]. The last term in (1) is the displacement current at the ith barrier where the potential drop is V_i and ϵ is the static permittivity.

1

Our numerical simulations (of the $3N+8$ coupled equations) have been performed for a 13.3 nm GaAs/2.7 nm AlAs SL at zero temperature consisting of 50 wells and 51 barriers, as described in [12]. Doping in the wells and in the contacts are $N_w = 2 \times 10^{10}$ cm^{-2} and $N_c = 2 \times 10^{16}$ cm^{-3} respectively. Notice that the typical experimental value is $N_c = 2 \times 10^{18}$ cm^{-3} [7,12]. For this value, we find current self-oscillations due to monopole dynamics with very small superimposed current spikes. Since the origin of such spikes is the same as for smaller N_c (for which spikes are larger and bistability of oscillations is possible), we choose not to present data comparable to experiments in this paper (see Ref. [12] for the relevant experimental data).

2. Monopole-mediated self-oscillations of the current. Fig. 1(a) depicts the current as a function of time for a dc bias voltage of 5.5 V on the second plateau of the SL $I-V$ characteristic curve. $J(t)$ oscillates periodically at 20 MHz. Between each two peaks of $J(t)$, we observe 18 additional spikes. The electric field profile is plotted in Fig. 1(b) at the four different times of one oscillation period marked in Fig. 1(a). There are two domains of almost constant electric field separated by a moving domain wall of (monopole) charge accumulation (which is extended over a few wells). Monopole recycling and motion occur on a limited region of the SL (between the 30th and the 50th well) and accompany the current oscillation [7,8]. Well-to-well hopping of the domain wall is reflected by the current spikes until it reaches the 46th well which is close to the collector. Then the strong influence of the contact causes that no additional spikes appear. Instead the current rises sharply triggering the formation of a new monopole closer to the emitter contact but well inside the SL; see Figs. 1(a) and (b). The number of wells traversed by the domain wall (almost) coincides with the number of spikes per oscillation period, *a feature not found in previous models.* Fig. 1(b) shows the recycling of a monopole: between times (1) and (3) there is a single monopole propagating towards the collector; at (4) a new monopole is generated at the middle of the structure and the old one collapses at the collector. It is interesting to realize that the region near the emitter does not have a constant electric field profile due to the large doping there (its Fermi level is well above the first resonant level of the first well). This produces a large accumulation layer.

3. Current spikes. What is remarkable in Fig. 1(a) (as compared to previous studies) are the spikes superimposed near the minima of the current oscillations. Such spikes have been observed experimentally and attributed to well-to-well hopping of the domain wall [12,15]. They are a cornerstone to interpret the experimental results and in fact support the theoretical picture of monopole recycling in part (about 40%) of the SL during self-oscillations. The identification between number of spikes and of wells traversed by the monopole rests on voltage turn-on measurements supported by numerical simulations of simple models during early stages of station-

ary domain formation [15]. These models do not predict spikes superimposed on current self-oscillations due to monopole motion [4,7,16]. To predict large spikes, a time delay in the tunneling current [12] or random doping in the wells [17] have to be added. Unlike these models, ours reproduces and explains spikes naturally thereby supporting their use to interpret experimental results.

Fig. 2(a) depicts a zoom of the spikes in Fig. 1(a). They have a frequency of about 500 MHz and an amplitude of 2.5 μA. Fig. 2(b) shows the charge density profile at four different times of a current spike marked in Fig. 2(a). Notice that the electron density in Fig. 2(b) is larger than the well doping at only three wells (40, 41 and 42) during the times recorded in Fig. 2(a). The maximum of electron density moves from well 40 to well 41 during this time interval so that: (i) tunneling through the 41st barrier (between wells 40 and 41) dominates when the total current density is increasing, whereas (ii) tunneling through barriers 41 and 42 is important when $J(t)$ decreases. The contributions of tunneling and displacement currents to $J(t)$ in Eq. (1) are depicted in Figures 2(c) and (d).

More generally, the spikes reflect the two-stage hopping motion –fast time scale– of the domain wall: at time (1) (minimum of the current), the charge accumulates mainly at the *i-th* well. As time elapses, electrons tunnel from this well to the next one, the *(i+1)-st*, where most of the charge is located at time (3) (maximum of current). This corresponds to a hop of the monopole. As the monopole moves, it leaves a lower potential drop on its wake. The reason is that the electrostatic field at the *(i+1)-st* well and barrier become abruptly flat between times (1) and (3), as they pass from the high to the low field domain. This means that a negative displacement current has its peak at the *(i+1)-st* barrier, near the wells where most of the charge is. Between times (1) and (3), the tunneling current is maximal where the displacement current is minimal and the total current increases. After that, some charge flows to the next well [time (4)] but both, tunneling and displacement currents, are smaller than previously. This occurs because the potential drop at barrier *(i+2)* (in the high field domain) is larger than at barrier *(i+1)*. Then there is a smaller overlap between the resonant levels of nearby wells –the tunneling current decreases – and the displacement current and, eventually, $J(t)$ decreases. This stage lasts until well i is drained, and most of the charge is concentrated at wells *(i+1)* (the local maximum of charge) and *(i+2)* (slightly smaller charge). Then the next current spike starts.

4. Dipole self-oscillations of the current. An advantage of our present model over other discrete ones [4,16,18] is our microscopic modeling of boundary conditions at the contact regions. Thus we can study what happens when contact doping is changed. The result is that there appear dipole-mediated self-oscillations as the emitter doping is lowered below a certain value. There is a range of voltages for which dipole and monopole oscillations coexist as stable solutions. This range changes for different plateaus. When the emitter doping is further lowered,

only the dipole self-oscillations remain. Fig.3 presents data in the crossover range (below $N_c = 4.1 \times 10^{16} \mathrm{cm}^{-3}$ and above $N_c = 1.7 \times 10^{16} \mathrm{cm}^{-3}$ for the second plateau), for the same sample, doping and bias as in Figs. 1 and 2. Except for the presence of spikes of the current, dipole recycling and motion in SLs are similar to those observed in models of the Gunn effect in bulk GaAs [13]. These self-oscillations have not been observed so far in experiments due to the high values of the contact doping adopted in all the present experimental settings. Notice that current spikes appear differently than in the monopole case, Fig. 1(a). The main difference is that now there are many more current spikes, 36, for the dipoles recycle at the emitter and traverse the whole SL. See Figs. 3(b) and (c). Charge transfer and balance between tunneling and displacement current during a spike are similar to those occurring in monopole oscillations. For a simpler model [4,8] the velocity of a charge accumulation layer (belonging to a monopole or a dipole) has been shown to approximately obey an equal area rule. Then monopole and dipole velocities are similar but a monopole traverses a smaller part of the SL than a dipole does. Therefore dipole oscillations have a lower frequency than monopole ones. Our results agree with this: the frequency of the dipole oscillations discussed above is about 8 MHz, 40% the frequency of monopole oscillations.

Dipole self-oscillations have also been predicted to occur in weakly-coupled SLs as the result of assuming a linear current – field relation at the injecting contact on a simpler model [16,19]. Since such *ad hoc* boundary condition has no clear relation to contact doping, no crossover between different oscillation types could appear in that work.

5. Multistability. Monopole and dipole waves coexist in both the first and the second plateaus. The time-averaged current as a function of dc voltage in the first plateau (whose crossover range is below $N_c = 2.1 \times 10^{16} \mathrm{cm}^{-3}$ and above $N_c = 1.5 \times 10^{16} \mathrm{cm}^{-3}$) has been plotted in Fig. 4. Notice that the average current of dipole oscillations is lower than that of monopole oscillations. Previous studies for Gunn oscillations [13] found that large dipole waves appear only for small current values, whereas monopole recycling requires current values near the maximum of the current-field characteristic curve. Let us start at a bias of 0.5 V (for which the stationary state is stable) and adiabatically increase the voltage. The result is that we go smoothly from the stationary state to the fast monopole self-oscillation at about 1.3 V. This branch of oscillatory states eventually disappears at about 2.6 V. If we now adiabatically lower the bias, we reach a slow dipole self-oscillation at about 2.4 V. There is a small hysteresis loop between dipole oscillations and the stationary state between 2.4 V and 2.6 V: the former may start as a subcritical Hopf bifurcation. About 0.8 V the dipole oscillation disappears and we are back at the stable stationary state. We therefore find the hysteresis loops marked by arrows in Fig. 4.

In conclusion, we have dealt with self-sustained os-cillations of the current in SLs whose main mechanism is sequential tunneling. Depending on contact doping, these oscillations may be due to recycling and motion of two different charge density waves: monopoles and dipoles. Experimentally, only the monopole oscillations have been observed, for the contacts doping is usually set to values which are too high. The dipole-like oscillations could be observed constructing samples with lower doping at the contacts. In fact, as the doping of the contacts is reduced, we predict current oscillations due to dipole charge waves. The crossover between both types of self-oscillations occurs at intermediate emitter doping values for which stable monopole and dipole oscillations coexist. Then the diagram of average current versus voltage is multivaluated, presenting hysteresis cycles and multistability between monopole and dipole oscillations (and between oscillatory and stationary states). The time-resolved current in the oscillatory modes presents a number of sharp spikes. They occur because well-to-well hopping of charge accumulation layers occurs in two stages: during the stage where the current rises, charge is mainly transferred through a single barrier. The charge is transferred through two adjacent barriers at the stage in which the current decreases. All these properties form the basis for possible applications of SLs working as multifrequency oscillators in a wide range of frequencies. Quantitative description of such multifrequency oscillators requires calculation of typical output power characteristics and noise levels. This is the purpose of a future work.

[1] *The Physics of Instabilities in Solid State Electron Devices*, M. P. Shaw, V. V. Mitin, E. Schöll and H. L. Grubin (Plenum Press, New York, 1992)
[2] K. K. Choi *et al*, Phys. Rev. B **35**, 4172 (1987).
[3] H. T. Grahn *et al*, Phys. Rev. Lett. **67**, 1618 (1991).
[4] L. L. Bonilla, in *Nonlinear Dynamics and Pattern Formation in Semiconductors and Devices*, edited by F.-J. Niedernostheide (Springer-Verlag, Berlin, 1995), page 1.
[5] J. Kastrup *et al*, Appl. Phys. Lett. **65**, 1808 (1994).
[6] R. Merlin *et al*, in *Proc. 22nd ICPS*, ed. D. J. Lockwood (World Scientific, 1995), p. 1039.
[7] J. Kastrup *et al*, Phys. Rev. B **55**, 2476 (1997).
[8] L. L. Bonilla *et al*, SIAM J. Appl. Math. **57**, 1588 (1997).
[9] O. M. Bulashenko and L. L. Bonilla, Phys. Rev. B **52**, 7849 (1995); O. M. Bulashenko, M. J. García and L. L.

Bonilla, *ibid.* **53**, 10 008 (1996).

[10] Y. Zhang *et al*, Phys. Rev. Lett. **77**, 3001 (1996).

[11] K. J. Luo *et al*, Phys. Rev. Lett. **81**, 1290 (1998).

[12] J. W. Kantelhardt *et al*, Physica Status Solidi B **204**, 500 (1997).

[13] F. J. Higuera and L. L. Bonilla, Physica D **57**, 161 (1992).

[14] R. Aguado *et al*, Phys. Rev. B **55**, R16053 (1997).

[15] J. Kastrup *et al*, Phys. Rev. B **53**, 1502 (1996).

[16] A. Wacker, in *Theory and transport properties of semi-conductor nanostructures*, edited by E. Schöll. (Chapman and Hill, New York, 1998), chapter 10.

[17] F. Prengel *et al*, in *Proc. 23rd ICPS*, ed. M. Scheffler and R. Zimmermann (World Scientific, 1996), p. 1667.

[18] F. Prengel, A. Wacker and E. Schöll, Phys. Rev. B **50**, 1705 (1994).

[19] L. L. Bonilla, E. Schöll and A. Wacker (1998), unpublished.

FIG. 2. (a) Zoom of Fig. 1 showing the spikes of the current. (b) Electron density profiles (in units of the doping at the wells), (c) tunneling current, and (d) displacement current within the monopole at the times marked in (a).

FIG. 3. (a) Dipole-mediated self-oscillations of the current at $5.5V$ for $N_c = 2 \times 10^{16}$ cm^{-3}. (b) Detail of the current spikes. (c) Electric field profiles at the times marked in (a).
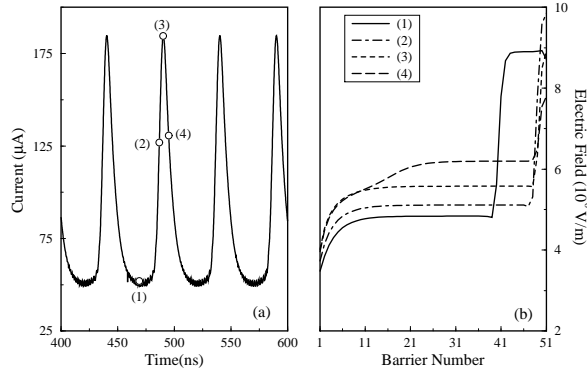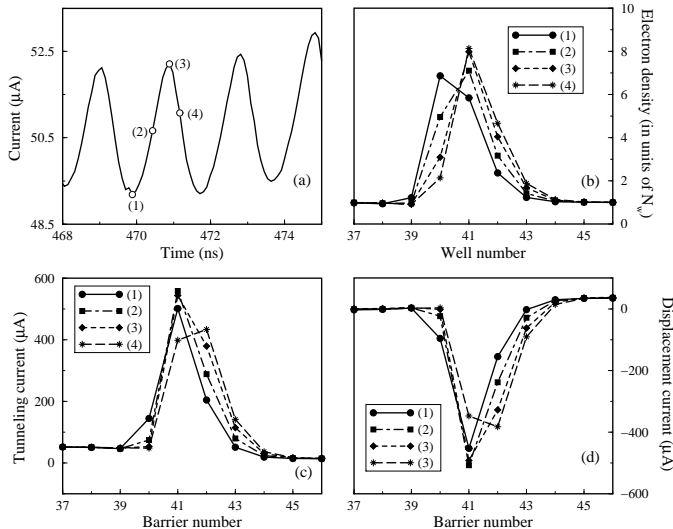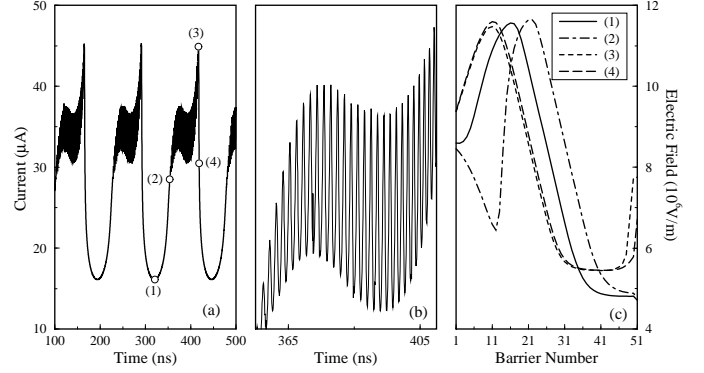

FIG. 1. (a) Self-sustained oscillations of the total current through the SL due to monopole recycling and motion. Bias is $5.5V$ and emitter doping, $N_c = 2 \times 10^{16}$ cm^{-3}. (b) Electric field profiles at the times marked in (a) during one period of the current oscillation.
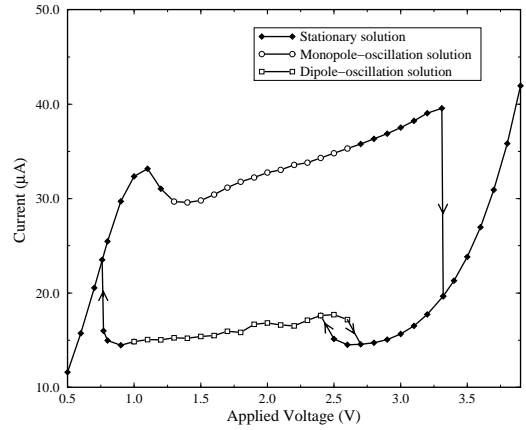

FIG. 4. I-V characteristics at the first plateau, for both sweep directions showing bistability between self-oscillations mediated by monopole and by dipole dynamics. Notice the hysteresis cycle.